COLD FORMING HOT-ROLLED WIDE FLANGE BEAMS INTO ARCHES
Preliminary finite element simulations

R.C. Spoorenberg, H.H. Snijder, J.C.D. Hoenderkamp, M.C.M. Bakker

Eindhoven University of Technology, Department of Architecture, Building and Planning, Eindhoven, the Netherlands

INTRODUCTION

Arches are structures curved in elevation, which carry vertical loads to the supports mainly by compressive action of the arch-rib. Their main application is in bridges and large span roofs of buildings. Arches made from hot-rolled wide flange sections can be cold formed by roller bending, *Fig. 1* and *Fig. 2*. This forming process affects the structural properties of the section which may have an influence on the structural behaviour of steel arches. The cold bending process induces change in residual stresses, dimensions of the cross section and material properties of the curved section compared to the straight section. This paper describes a first attempt to investigate these effects by means of a finite element model. The accuracy of the finite element model is compared to experiments performed earlier [1].

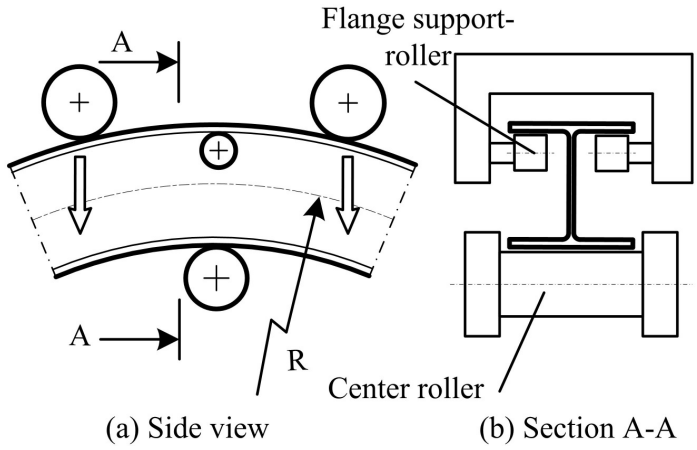

Fig. 1 Roller bending process

Fig. 2 Roller bent arch (HE 100A)

1 STATE OF THE ART

To date no study has been published on numerical modelling of the influence of the roller bending process on the properties of wide flange sections. Past numerical investigations have focused on the bending process with respect to the fabrication procedure [2], the influence of the rotary draw bending process on steel sections [3], the effects of the three point bending process on cold-formed sections [4] and the effect of coiling and uncoiling of wide sheet steel [5]. For an investigation into the lateral torsional behaviour of arch structures the influence of the roller bending process on structural properties of hot-rolled HE 100A sections was determined experimentally at the Eindhoven University of Technology [1] [6].

2 FINITE ELEMENT MODELING

A general purpose finite element program, ANSYS, release 11.0, has been used to simulate the effects of the roller bending process. The actual roller bending process includes friction and changing contact points between rollers and beam. The beam is curved by forced deformation, introducing shear and bearing stresses in the beam. As a first step to simulate the effects of the roller bending process it is investigated whether it is sufficiently accurate to model the roller bending process by prescribing a constant curvature of the beam, thus neglecting the influence of

friction, shear forces and bearing stresses. The section of the specimen is modelled with shell elements with seven integration points through the thickness. The shell element contains 4 nodes with 6 degrees of freedom per node and is based on the Mindlin-Reisnner theory. Twenty four elements were employed over the height *h* of the web and eight elements over the width *b* of the flange (*Fig. 3a*) to capture the residual stress distribution. Corner radii were not modelled. A steel HE 100A section was modelled with one end fixed and the other end free (*Fig. 3b*). To reduce computation time only 1/20 of the total developed length of arch has been modelled (*Fig.3c*). At the fixed end, all nodes were constrained in the longitudinal direction and perpendicular to the plane of the web. In addition, the node at mid-depth was constrained also in the direction perpendicular to the plane of the flange. In order to prevent lateral-torsional buckling, the beam was laterally supported at both web-flange junctions. The deformations of the flange perpendicular to the flange were coupled over the width of the flange in order to prevent flange buckling and indirectly web buckling. End-effects were prevented by applying stiff beam elements at the outer ends of the model.

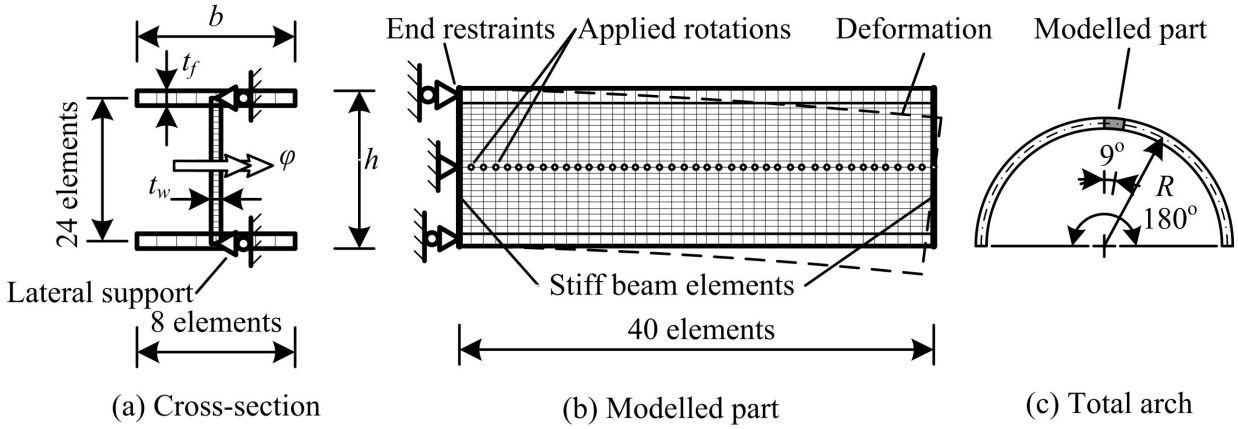

Fig. 3 FE-model

Cold bending was achieved by specifying a rotation φ at the reference nodes at mid-depth along the member, corresponding to the desired curvature (*Fig. 3b*), thereby taking into account springback. This enables the shift of the neutral axis towards the compressive side, which occurs in sheets and beams subjected to severe bending [7]. However, the position of the neutral axis of the beam during the roller bending process is not known. Two steps were required to simulate the complete roller bending process: cold bending was simulated by applying the prescribed rotations and springback was simulated by releasing these prescribed rotations. Three arches were modelled. The cross-sectional dimensions and the arch dimensions [1] are shown in *Table 1* and *Table 2* respectively. Geometrical and physical non-linearities were taken into account. The steel was assumed to be elasto-plastic with a stress-strain relationship based on standard tensile load tests on coupons from the straight hot-rolled sections [1]. The material model was characterized by the Von Mises yield criterion and the Prandtl-Reuss flow rule with hardening.

Table 1. Dimensions of cross-sections before cold forming [1]

Arch number	h [mm]	$b_{top} = b_{bot}$ [mm]	t_w [mm]	$t_{f;top} = t_{f;bot}$ [mm]
1,2,3	96.92	100.76	5.36	7.72

3 RESULTS

The investigation has been focused on the following items: changes in cross-sectional dimensions, residual stress distribution and mechanical properties. In all three numerical simulations of the cold bending process it was found that a shift of the neutral axis towards the compressive side occurred, with a maximum shift of 5 mm.

3.1 Change of cross-sectional dimensions

The cross sectional dimensions after bending are presented in *Table 2*. The cross-sectional change was obtained with the use of a sliding calliper and a micrometer. Column 3 shows the dimensions obtained from previous experiments [1]. The numerical results are given in column 4. The change in dimensions between cross-sections of the straight member and the arched structures are presented in column 5 and column 6 respectively. The percentage difference in dimensional change between the experimental and numerical results is shown in column 7, for which: Diff=(ΔExp-ΔNum)/ΔExp.

Table 2. Arch dimensions and cross-sectional dimensions after bending

1	2	3	4	5	6	7
	Item	Experimental [1] [mm]	Numerical [mm]	ΔExp. [mm]	ΔNum. [mm]	Diff [%]
Arch no. 1 R = 1910 [mm] Bending ratio R/h = 19.9	b_{top}	100.09	99.54	- 0.67	- 1.22	- 82 %
	b_{bot}	102.03	101.83	1.27	1.07	16 %
	h	96.09	96.78	- 0.83	- 0.14	83 %
	$t_{f;top}$	7.63	7.63	- 0.09	- 0.09	0 %
	$t_{f;bot}$	7.89	7.80	0.17	0.08	53 %
Arch no. 2 R = 2546 [mm] Bending ratio R/h = 26.5	b_{top}	100.2	99.85	- 0.56	- 0.91	- 63 %
	b_{bot}	101.66	101.55	0.90	0.79	12 %
	h	96.22	96.83	- 0.70	- 0.09	87 %
	$t_{f;top}$	7.60	7.65	-0.12	- 0.07	42 %
	$t_{f;bot}$	7.85	7.78	0.13	0.06	54 %
Arch no. 3 R = 3820 [mm] Bending ratio R/h = 39.8	b_{top}	100.50	100.18	- 0.26	- 0.58	- 123 %
	b_{bot}	101.44	101.28	0.68	0.52	24 %
	h	96.33	96.86	- 0.59	- 0.06	90 %
	$t_{f;top}$	7.64	7.68	-0.08	- 0.04	50 %
	$t_{f;bot}$	7.87	7.76	0.15	0.04	73 %

3.2 Development of residual stresses

The cold bending process introduces residual stresses into the cross section. These residual stresses are different in pattern and magnitude compared to residual stresses due to non-uniform cooling of hot-rolled members. The cold bending residual stresses are a summation of the axial stresses due to plastic bending and elastic unloading of the cross section (*Fig. 4*). The residual stresses in the web obtained from the numerical analyses and experiments are shown in *Fig. 6*. The residual stresses were measured by employing the hole-drilling method [1].

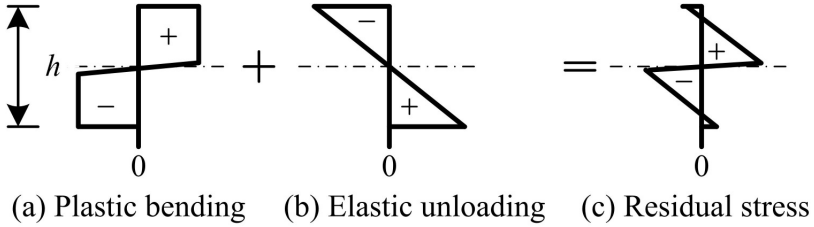

(a) Plastic bending (b) Elastic unloading (c) Residual stress

Fig. 4 Residual stresses due to roller bending

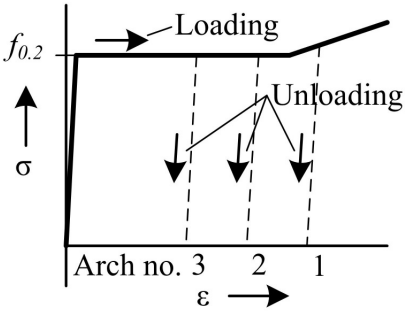

Fig. 5 Straining of the arches due to bending process.

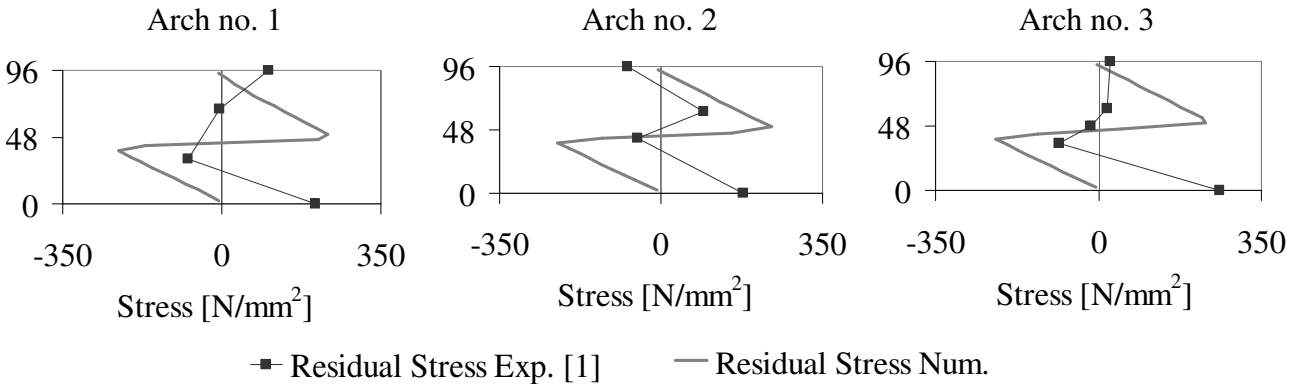

Fig. 6 Residual stresses along the height of the web

3.3 Change of material properties

The cold straining to which steel is subjected when formed into arches affects the mechanical properties. Generally cold straining is accompanied by an increase in yield strength, ultimate tensile strength and a decrease in ductility. The change in material properties can be obtained from the finite element simulations by reloading a single element of the original model after springback with a tensile force in the longitudinal direction. The altered yield strength ($f_{0.2}$) and ultimate tensile strength (f_t) can then be obtained [8]. The numerical simulations are compared to previous tensile tests on coupons taken from the top flange and bottom flange of a cold bent arch. The yield strength is defined as the 0.2 % proof strength when a yield plateau is absent. The experimental data were obtained at three different locations along the width of the flange. For simplicity these three values are averaged. The numerical data were found to be constant over the width of the flange.
The experimental and numerical results for the top flange of the three arches are presented in *Table 3* and *Fig. 7*. The dashed line shows the 0.2 % proof strength and ultimate tensile strength of the original material. The difference between the experimental and numerical results is defined by: Diff = (Exp –Num)/ Exp. Since the direction of reloading is identical to the direction of cold straining the Bauschinger effect has no influence on the hardening behaviour.

Table 3. The 0.2 % proof strength ($f_{0.2}$) and ultimate tensile strength (f_t) of top flanges

Arch no.	Experimental [1] [N/mm^2]		Numerical [N/mm^2]		Difference [%]	
	$f_{0.2}$	f_t	$f_{0.2}$	f_t	$f_{0.2}$	f_t
1	290	423	298	413	2.75	-2.36
2	303	423	283	413	-6.60	-2.36
3	287	415	270	408	-5.92	-1.69

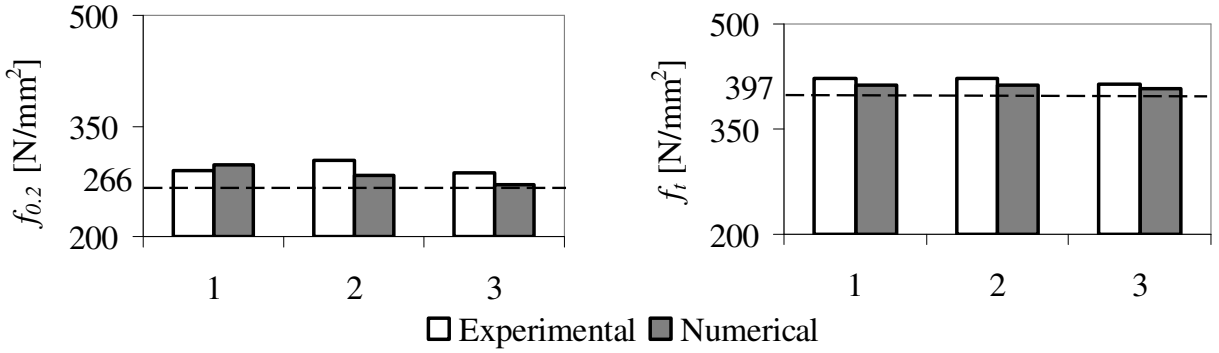

Fig. 7. The 0.2 % proof strength ($f_{0.2}$) and ultimate tensile strength (f_t) of top flanges.

The bottom flange is subjected to compressive action due to cold bending. The influence of the Bauschinger effect has been studied in the numerical model by employing either a kinematic or an isotropic hardening law; see *Table 4* and *Fig. 8*. The first hardening law fully incorporates the Bauschinger effect; the latter completely ignores the Bauschinger effect [9]. Since the amount of straining is outside the hardening range for arch 2 and 3 (*Fig. 5*) the influence of the Bauschinger effect is smaller for these arches.

Table 4. The 0.2 % proof strength ($f_{0.2}$) and ultimate tensile strength (f_t) of bottom flanges

Arch no.	Experimental [1] [N/mm^2]		Numerical [N/mm^2]				Difference [%]			
			Kinematic		Isotropic		Kinematic		Isotropic	
	$f_{0.2}$	f_t	$f_{0.2}$	f_t	$f_{0.2}$	f_t	$f_{0.2}$	f_t	$f_{0.2}$	f_t
1	307	417	249	389	286	406	-18.9	-6.71	-6.84	-2.64
2	303	431	261	393	274	405	-13.9	-8.82	-9.57	-6.03
3	249	410	263	394	267	404	5.62	-3.90	7.23	-1.46

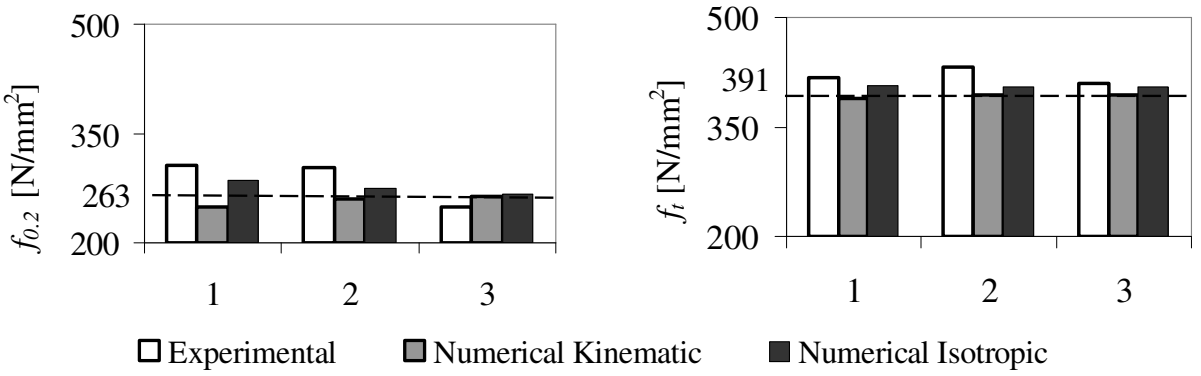

Fig. 8. The 0.2 % proof strength ($f_{0.2}$) and ultimate tensile strength (f_t) of bottom flanges.

4 CONCLUSIONS

4.1 Suitability of finite element model

It has been shown that a simple finite element model comprising shell elements only is able to give altered properties resulting from a cold forming process. Based on the rather limited number of simulations it is not possible to conclude at this stage whether the proposed model is capable of describing the effects of roller bending on wide flange sections with reasonable accuracy. More experimental data of various arches are needed to investigate the accuracy of the finite element model. Also it must be recognized that the experimental results may contain inaccuracies. Some comments can be made on the observed tendencies.

4.2 Cross-sectional dimensions

It has been shown that an increase of the bending ratio reduces the change in dimensions of the cross section. This tendency is confirmed by all numerical simulations, and by all experiments, with the exception of the flange thickness of arch 2. The change of width of the top flange by numerical analyses is larger than in the experiments. However, the reverse is true for the change of height, width of the bottom flange and thickness change in top and bottom flange. This could be due to the absence of bearing and shear forces in the numerical simulations which are present in the actual forming process.

4.3 Residual stresses

The residual stresses in the web show qualitative agreement with the theoretical solution [10], but do not agree well with the experimentally obtained values. The bending ratio has little effect on the distribution and magnitude of the residual stress pattern along the height of the web, as can be seen in *Fig. 6*. This is attributed to the fact that the strains due to cold bending are so small that the material is not stretched outside the hardening range, as depicted in *Fig. 5*. This results in an almost identical springback for all three arches.

4.4 Material properties

The numerical model is capable to display the tendencies of the bending process with respect to the material law (e.g. a larger increase in yield strength and ultimate tensile strength is found for a decreasing radius). Though, it can be observed that the experimentally obtained increase of yield strength and ultimate tensile strength are considerably larger than the numerical results. The experimental results however, do not show a consistent correlation between the bending ratio and the increase of yield strength and ultimate tensile strength; see *Fig. 7* and *Fig. 8*.

5 ACKNOWLEDGEMENTS

This investigation has been performed under projectnumber MC1.06262 in the framework of the Strategic Research Programme of the Netherlands Institute for Metals Research (www.nimr.nl).

REFERENCES

[1] La Poutre, D. B. (2004). *Inelastic Spatial Stability of Circular Wide Flange Steel Arches*: PhD-thesis, Technische Universiteit Eindhoven. Eindhoven; The Netherlands: 188 p.

[2] Hansen, N. E. & Jannerup, O. (1979). Modeling of elastic-plastic bending of beams using a roller bending machine. *J. Eng. Ind-T ASME*, 101(3), 304-310

[3] Welo, T., Paulsen, F., & Brobak, T. J. (1994). The Behaviour of Thin-Walled, Aluminium Alloy Profiles in Rotary Draw Bending - A Comparison between Numerical and Experimental Results. *Journal of Materials Processing Technology*, 45, 173-180

[4] Zhao, K. M. & Lee, J. K. (2002). Finite element analysis of the three-point bending of sheet metals. *Journal of Materials Processing Technology*, 122, 6-11

[5] Quach, W. M., Teng, J. G., & Chung, K. F. (2004). Residual stresses in steel sheets due to coiling and uncoiling: a closed-form analytical solution. *Eng. Struct.*, 26(9), 1249-1259

[6] La Poutre, D. B., Snijder, H. H., Hoenderkamp, J. C. D., & Bakker, M. C. M. (2004). Effects of the bending process on the out-of-plane stability of steel arches. *Annual technical session & meeting SSRC annual stability conf.*

[7] Hill, R. (1950). *The Mathematical Theory of Plasticity*. London: Oxford University Press. 355 p.

[8] Spoorenberg, R. C., Snijder, H. H., & Bakker, M. C. M. (2008). *Cold Forming of Arched Hot-rolled Wide Flange Beams with Finite Element Simulations: Research Report No 0-2008-5*. Eindhoven; the Netherlands: Eindhoven University of Technology, Department of Architecture, Building and Planning.

[9] Tan, Z., Magnusson, C., & Persson, B. (1994). The Bauschinger effect in compression-tension of sheet metals. *Materials Science and Engineering*, 183, 31-38

[10] King, C. & Brown, D. (2001). *Design of Curved Steel*. Berkshire: The Steel Construction Institute. 112 p.